AGU PUBLICATIONS

Geophysical Research Letters

RESEARCH LETTER
10.1002/2016GL069755

Key Points:
- Tectonic tremor in Cascadia modulated by teleseismic waves of the 2012 Indian Ocean earthquake
- The rate of tremor activity increased by 1.5 times from its background level
- Both body and surface waves modulate ongoing tremor activity

Supporting Information:
- Supporting Information S1
- Figure S1
- Figure S2

Correspondence to:
B. Kundu,
rilbhaskar@gmail.com

Citation:
Kundu, B., A. Ghosh, M. Mendoza, R. Bürgmann, V. K. Gahalaut, and D. Saikia (2016), Tectonic tremor on Vancouver Island, Cascadia, modulated by the body and surface waves of the M_w 8.6 and 8.2, 2012 East Indian Ocean earthquakes, *Geophys. Res. Lett.*, *43*, doi:10.1002/2016GL069755.

Received 26 MAY 2016
Accepted 24 AUG 2016
Accepted article online 26 AUG 2016

©2016. American Geophysical Union. All Rights Reserved.

Tectonic tremor on Vancouver Island, Cascadia, modulated by the body and surface waves of the M_w 8.6 and 8.2, 2012 East Indian Ocean earthquakes

Bhaskar Kundu[1], Abhijit Ghosh[2], Manuel Mendoza[2], Roland Bürgmann[3], V. K. Gahalaut[4], and Dipankar Saikia[5]

[1]Department of Earth and Atmospheric Sciences, NIT Rourkela, Rourkela, India, [2]Department of Earth Sciences, University of California, Riverside, California, USA, [3]Department of Earth and Planetary Science, University of California, Berkeley, California, USA, [4]National Centre for Seismology, Ministry of Earth Sciences, New Delhi, India, [5]Indian National Centre for Ocean Information Services, Hyderabad, India

Abstract The 2012 East Indian Ocean earthquake (M_w 8.6), so far the largest intraoceanic plate strike-slip event ever recorded, modulated tectonic tremors in the Cascadia subduction zone. The rate of tremor activity near Vancouver Island increased by about 1.5 times from its background level during the passage of seismic waves of this earthquake. In most cases of dynamic modulation, large-amplitude and long-period surface waves stimulate tremors. However, in this case even the small stress change caused by body waves generated by the 2012 earthquake modulated tremor activity. The tremor modulation continued during the passage of the surface waves, subsequent to which the tremor activity returned to background rates. Similar tremor modulation is observed during the passage of the teleseismic waves from the M_w 8.2 event, which occurs about 2 h later near the M_w 8.6 event. We show that dynamic stresses from back-to-back large teleseismic events can strongly influence tremor sources.

1. Introduction

Since the discovery of tectonic tremors [*Obara*, 2002], accumulating high-precision data suggest that tremors are composed of many overlapping events, individually called low-frequency earthquakes (LFEs) [*Shelly et al*., 2007, 2011]. In addition, very low frequency earthquakes are associated with tremor activity and release significant amount of seismic moment during major tremor episodes [*Ghosh et al*., 2015]. Episodic tremor and associated slow slip or episodic tremor and slip (ETS) events occur in the transition zone between the seismogenic, locked plate-boundary fault to the deeper aseismically slipping plate-interface in diverse tectonic settings [*Peng and Gomberg*, 2010]. Each individual LFE represents shear slip that is too small to detect geodetically, but the largest ETS events can be resolved geodetically, showing that the tremors illuminate extensive slow-slip episodes on the plate interface [*Ide et al*., 2007; *Bartlow et al*., 2012]. For example, along the northern Cascadia subduction zone, the largest ETS events rupture areas of up to ~50 km by ~300 km with only a few centimeter of slip, approximately every ~14 months [*Bartlow et al*., 2012]. From a seismic hazard perspective, ETS events are important as they may transfer stress to the updip seismogenic plate interface with a potential to trigger a megathrust earthquake [*Dragert et al*., 2004; *Mazzotti and Adams*, 2004; *Wech and Creager*, 2011]. More specifically, the seismogenic plate interface may experience a discrete increase in stress with each individual ETS [*Wech and Creager*, 2011]. In fact, a large tremor episode was found to trigger small earthquakes located near the plate interface in Cascadia and New Zealand [*Delahaye et al*., 2009; *Vidale et al*., 2011].

Tremor activity shows transient modulation in response to earth tides [*Thomas et al*., 2013; *Thomas et al*., 2009; *Hawthorne and Rubin*, 2010] and the passage of radiating seismic waves from distant earthquakes [*Ghosh et al*., 2009; *Gomberg*, 2010; *Shelly et al*., 2011]. It is characterized by noise-like emergent waveforms, predominantly devoid of high-frequency energy compared to regular earthquakes. Tremor durations range from a few seconds to days with waveform envelopes that are coherent across many seismic stations miles apart. Nonvolcanic tremor and low-frequency earthquakes have been reported in both subduction zones and transform plate boundary regions around the world [*Peng and Gomberg*, 2010; *Peng and Gomberg*, 2010; *Shelly et al*., 2011]. Besides the SW-Japan region [*Obara et al*., 2004], the Cascadia subduction zone in the Pacific Northwest of North America is probably the best instrumentally monitored region for tremor and

ETS. The clearest and most emphatic dynamic triggering and tremor modulation is caused by the long-period Love and Rayleigh waves. So far, only a few cases have been reported of triggering/modulation due to body waves [*Ghosh et al*., 2009; *Shelly et al*., 2011; *Miyazawa*, 2012]. Specifically, the mechanism of tremor and its reaction to the dynamic stressing from various phases of body and surface waves are poorly understood. Here we scrutinize the modulation of seismic tremor in the Cascadia subduction zone by the 11 April 2012 M_w 8.6 East Indian Ocean earthquake (Figure 1a), so far the largest intraoceanic plate strike-slip event ever recorded [*McGuire and Beroza*, 2012]. In Cascadia, the oceanic Juan de Fuca plate subducts below the North American plate between Mid-Vancouver Island and Northern California, at a relative convergence rate of ~4 cm/yr. The transition zone between the locked and aseismically slipping plate interface hosts the tremor activity. Along the Cascadia subduction zone ~2–3 cm of transient surface displacement due to major ETS events occurs over a period of ~3 weeks with recurrence intervals varying between 10 to 19 months [*Brudzinski and Allen*, 2007], interspersed by smaller quasi-continuous "inter-ETS" tremor sequences [*Ghosh et al*., 2012; *Wech and Creager*, 2011].

We observe that during the passage of seismic waves of the 2012 East Indian Ocean earthquake (M_w 8.6), the rate of tremor activity on Vancouver Island of northern Cascadia increased by more than 1.5 times from the ongoing tremor activity of a small tremor swarm (Figures 1b and 1c). The modulated tremor activity starts after the arrival of the shear body waves and continued during the passage of surface waves, after which it abruptly returned to background rates. The process is captured by the sensitive borehole strainmeter and seismograph network of the Plate Boundary Observatory (PBO) operated by University NAVSTAR Consortium (UNAVCO), broadband seismogram data archived by the Canadian National Seismograph Network (CNSN), and tremor catalogue data from the Pacific Northwest Seismic Network (PNSN).

2. 11 April 2012 M_w 8.6 East Indian Ocean Earthquake

On 11 April 2012, at 08:38:37 UTC, a great intraoceanic plate strike-slip earthquake (M_w 8.6) occurred in the East Indian Ocean region on the Indo-Australian plate, about 200 km west of the Sumatra subduction zone. Two hours later, another earthquake (M_w 8.2) occurred about 180 km south of the main shock (Figure 1a). The main shock is probably the largest intraplate event ever recorded in the modern era of instrumental seismology [*McGuire and Beroza*, 2012]. It was a complex event, rupturing a series of subparallel (approximately north-south) and conjugate faults (Figure 1a) with predominant moment release in a 100–160 s time span [*Kiser*, 2012; *Wang et al*., 2012; *Meng et al*., 2012; *Yue et al*., 2012; *Pollitz et al*., 2012; *Ishii et al*., 2013]. Reported GPS-derived coseismic offsets [*Yadav et al*., 2013] are consistent with finite slip models derived from broadband body and surface waves recorded by the global networks [*Yue et al*., 2012]. These conjugate intraoceanic ruptures were encouraged by stress transfer from the 2004 Sumatra-Andaman and 2005 Nias earthquakes [*Delescluse et al*., 2012; *Wiseman and Bürgmann*, 2012]. *Pollitz et al*. [2012] reported that the 2012 intraoceanic plate earthquake remotely triggered a large number of earthquakes (including $M_w \geq 5.5$) worldwide. These earthquakes were preferably located in the four lobes of Love-wave radiation, and most of them occurred where the dynamic shear strain exceeded 10^{-7} for 100 s during dynamic wave propagation [*Pollitz et al*., 2012]. However, none of the 16 $M_w \geq 5.5$ trigger candidates during the first 6 days occurred before 14 h after the main shock, suggesting delayed triggering by aseismic deformation, fluid flow, or other transient processes [*Johnson and Bürgmann*, 2015; *Delorey et al*., 2015]. Reports of triggered tremor activity from the M_w 8.6 event include the Kyushu, Nankai, Kanto, and Hokkaido regions in Japan [*Chao and Obara*, 2015] and near Queen Charlotte Island, Canada [*Aiken et al*., 2013].

3. Modulated Tectonic Tremor in Vancouver Island, Cascadia

Figure 1c shows the tremor activity near Vancouver Island, which was modulated after the arrival of seismic waves from the 2012 M_w 8.6 East Indian Ocean earthquake. The increase in tremor activity started at around 09:11:10 UTC at a location which is different from the earlier triggered tremor sources [*Rubinstein et al*., 2007; *Rubinstein et al*., 2009; *Chao et al*., 2013]. We also observe that the rate of tremor activity significantly increased after the arrival of body waves of the 2012 earthquake. The time of first arrival (Pdiff) of teleseismic waves of the M_w 8.6, 2012 earthquake in this region (e.g., as seen at the PGC site of the CNSN network) is 08:53:37 UTC. The increase in tremor activity at around 09:11:10 UTC coincides with the arrival of shear body waves and lasted for about ~2 h during which body and surface waves of the M_w 8.6 event arrived (Figure 2).

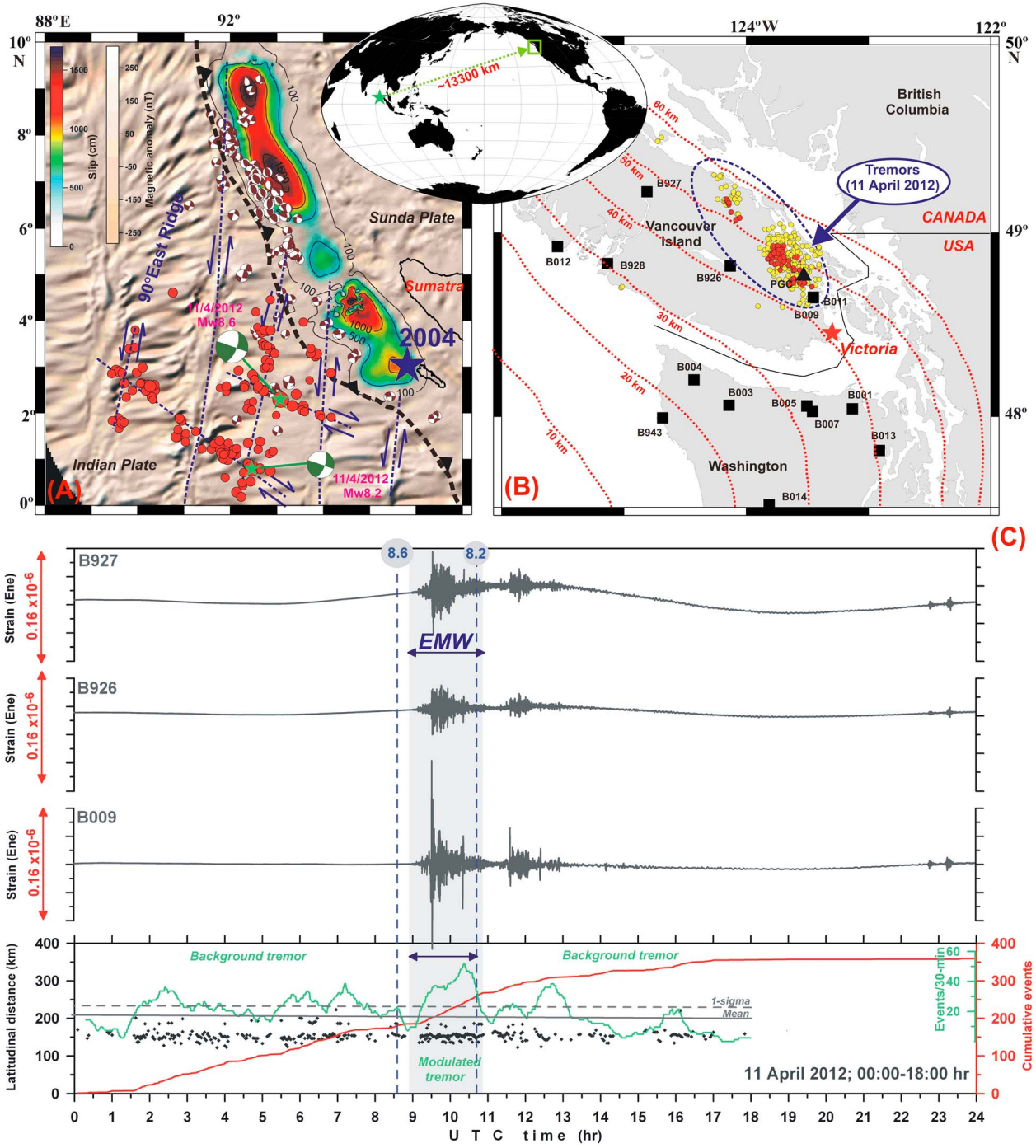

Figure 1. Tectonic tremor activity in the Cascadia subduction zone modulated by the 11 April 2012 East Indian Ocean earthquake. (a) Magnetic anomalies [http://geomag.org/models/wdmam.html] and general tectonics of Sumatra subduction zone and location of the 11 April 2012 East Indian Ocean earthquakes (M_w 8.6 and M_w 8.2). The 2004 Sumatra-Andaman earthquake rupture in the Sumatra frontal arc [*Chlieh et al.*, 2007] and its epicenter is also shown. Fracture zones are identified on the basis of swath bathymetry data [*Graindorge et al.*, 2008]. (b) The yellow filled circles are the catalogued tectonic tremors near Vancouver Island that occurred on the day of the 11 April 2012 East Indian Ocean earthquake. Tremor locations are taken from pnsn.org. The solid squares show the borehole strainmeters and seismometers of the Plate Boundary Observatory (PBO). The solid triangle denotes the broadband station, PGC, operated by the Canadian National Seismograph Network (CNSN). Isodepths of plate interface (at 10 km depth intervals) are also shown by red dashed lines [*Houston et al.*, 2011]. (c) Temporal variations of shear strain (Ene) at the three nearest PBO borehole stations (B009, B926, and B927) are shown in the upper three panels. The blue dashed lines are the origin times of the two earthquakes. The bottom figure shows the origin time of tremors (black dots) and cumulative number of tremor detections on Vancouver Island (red curve) on 11 April 2012. The rate of tremor activity in 30 min sliding window with 1 min shift is shown by green curve with the mean rate and 1σ value of tremor activity during the tremor swarm shown by horizontal solid and dashed lines, respectively. The red filled circles denote the tremors during effective modulation window (EMW) shown by gray shading in Figure 1c.

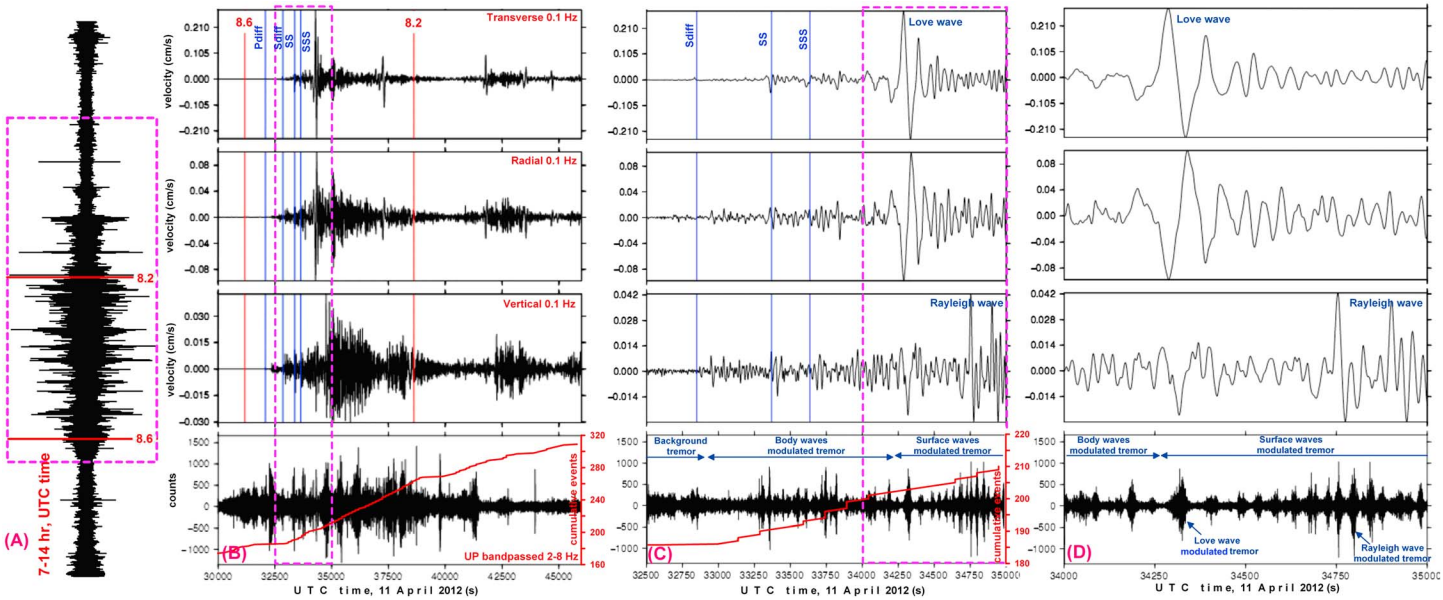

Figure 2. Waveforms recorded at a nearby seismic station PGC (location shown in Figure 1b). (a) Longer time window of 7 to 14 h UTC of 11 April 2012. (b–d) The magnified views (highlighted by dashed magenta boxes in Figures 2a–2c, respectively). The origin times of the two earthquakes are marked by the red lines, while the arrivals of various phases of teleseismic phases of the main shock (see labels in top figures) are marked by the blue lines. A 2–8 Hz band-pass butterworth filter was used. Note the cumulative number of catalogue tremor events (shown by red curve in Figure 2b and in Figure 1c), which increased after the arrival of body waves. Tremor signals are synchronous with the lower frequency and larger-amplitude phases of the body and surface waves of the 11 April 2012 East Indian Ocean earthquake.

We have defined the "effective-modulation window (EMW)" (marked by a gray bar in Figure 1c) as the time window bounded by the first Pdiff wave arrival (i.e., Pdiff = 08:53:37 UTC) and the final passage of major Rayleigh wave trains for the M_w 8.6 event (09:39:10 UTC). There appears to be a sudden jump in tremor activity (about 1.5 times of background tremor activity level) within the EMW (green curve in Figure 1c); however, it is not possible to uniquely distinguish between the modulated tremor and background tremor within the EMW (Figure 1c). Since tremor is ongoing even before the arrival of teleseismic waves, we refer to the pulses of tremor and its increased frequency within the EMW as modulated tremor activity.

The strainmeter records in Vancouver Island document the time and duration of the teleseismic wave arrivals, which lasted for about 4 h (Figure 1c). The maximum transient shear strain was 0.13×10^{-6} for the M_w 8.6 earthquake and 0.04×10^{-6} for the M_w 8.2 aftershock (Figure 1c). The tremor activity was recorded at three borehole seismometers co-located with the strainmeters, namely, B009, B011, and B926 (Figure S1 in the supporting information). Stations far away from the tremor location do not exhibit any tremor-like signal during this period. The accelerated tremor activity at the nearby stations was decayed to the initial background rate before the arrival of teleseismic waves of the M_w 8.2 aftershock (Figure S1).

We analyze the waveforms at the nearest broadband seismic station (PGC belonging to CNSN network) in further detail (Figure 2). The high-frequency waveforms (2–8 Hz) of modulated tremors at this station are synchronous with the lower frequency larger-amplitude arrivals of the body and surface waves of the 2012 East Indian Ocean earthquake (M_w 8.6). The modulated tremor activity (Figure 2) does not start instantaneously with the first arrival of the teleseismic wave (i.e., Pdiff) but initiate during the arrival of shear wave phases (between the arrival of Sdiff and SS), well before the arrival of surface waves of the M_w 8.6 event. The effective increase in the overall rate of catalogued tremor events is consistent with these observations (Figure 1c).

Enhanced tremor activity further continues during the passage of surface waves (i.e., both Rayleigh and Love waves). It is evident that the tremor sequence consistently tracked the high-amplitude phases of the surface waves (Figures 2c and 2d). The timing of onsets of tremor bursts is coincident with the large-amplitude phases of the earthquake waveform, which implies a modulating phenomenon. Another notable feature is the amplitude of tremors during the EMW. The amplitudes increase significantly above the background tremor amplitudes, suggesting much higher seismic energy release in tremor form within the EMW (Figure 2b). The tremor modulation continues during the passage of the surface waves, after which it was abruptly terminated and

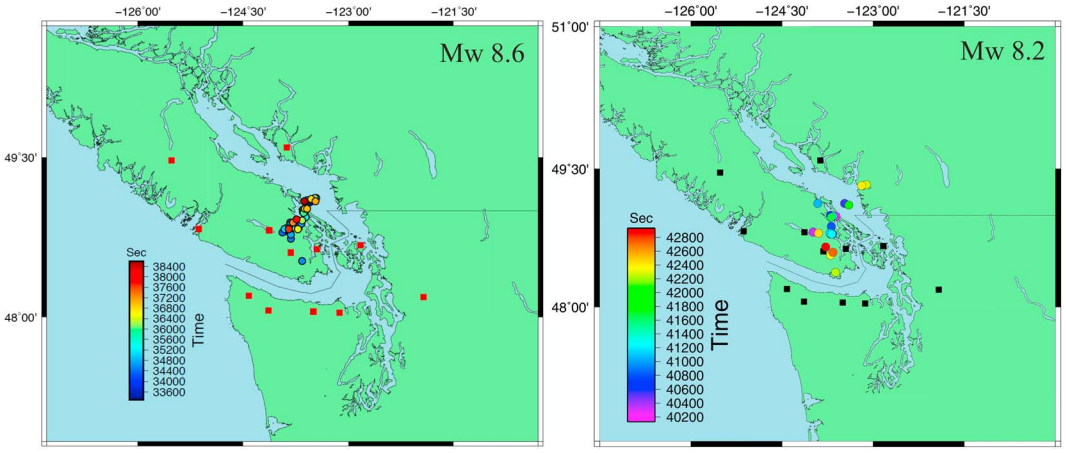

Figure 3. Modulated tremor in Cascadia during M_w 8.6 and M_w 8.2 events. Seismic stations (marked by squares) used to locate modulated tremor (circles colored by time) in Cascadia during M_w 8.6 and 8.2 events, respectively. A spatiotemporal map shows the high-quality tremor locations from time of *S* wave modulating to Rayleigh wave modulating.

the activity diminished to initial background rate. Tremor activity continues during the passage of teleseismic waves of the M_w 8.2 event, which occur about 2 h after the main shock. Tremor is clearly modulated by the teleseismic surface waves. During the passage of the *S* waves, tremor modulation is not as obvious although tremor activity is fairly strong. Because of the ongoing spontaneous tremor episode and lack of clear tremor modulation, it is difficult to assess if tremor activity is influenced by the teleseismic body waves from the M_w 8.2 event. However, we observe clear bursts of tremor during the passage of surface waves, particularly during Rayleigh waves (Figures 4 and S1). The inter-ETS swarm ended about 7 h later (Figures 1c and S1).

The above observations motivate us to further probe the tremor modulation process in detail. Using nearby stations' waveform data, we have located the modulated tremor in Cascadia (Figures 3 and 4). We only use stations with high signal-to-noise ratio. Interestingly, tremor is located in a linear fashion parallel to the slip

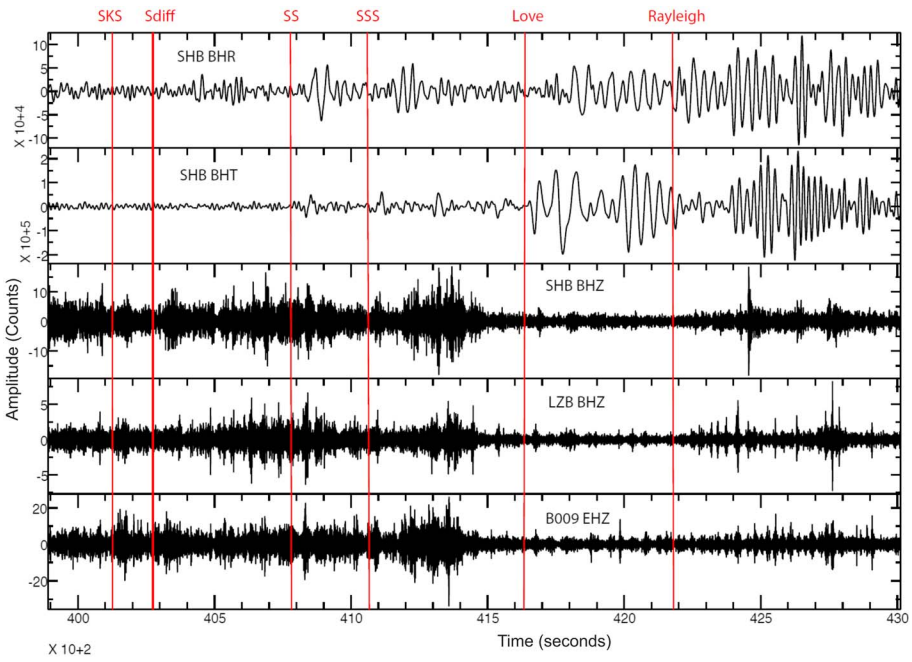

Figure 4. Teleseismic waves and associated tremor during the M_w 8.2 event. (first and second panels) Seismograms low-pass filtered at 10 s showing teleseismic waves. (third to fifth panels) Seismograms filtered between 2 and 8 Hz showing coherent tremor. Station names and components are indicated in each panel. Predicted arrival times of different teleseismic phases are marked by the red vertical lines.

direction of the subduction zone. It is generally consistent with the tremor locations determined by PNSN, although it does not resolve the linear feature. The tremor locations are organized as an elongated patch parallel to the slip vector. Similar slip-parallel tremor streaks have previously been reported in Cascadia [*Ghosh et al*., 2010]. However, it is not possible to resolve tremor movement at this scale using an envelope cross-correlation approach, and therefore, it is difficult to estimate direction of tremor streak propagation, speed etc. The strong slip-parallel linear alignment of tremor locations does suggest along dip streaking activity. This marks the first observation of tremor streaking in Cascadia associated with the passage of strong teleseismic waves. It perhaps indicates accelerated slow slip produced by the transient stress from teleseismic waves. This also suggests influence of transient stresses on the tremor activity. Interaction of propagating slow slip front with fault plane topography may have generated streaking tremor [*Ghosh et al*., 2010].

Modulation of tremor by body waves, which is relatively rare, is one of the most interesting observations of this study. Figure 5 shows that the tremor modulation is clear between the *S* waves and surface waves of the 2012 East Indian Ocean earthquake (M_w 8.6) and during the continued passage of teleseismic surface waves. Tremor during the passage of *S* waves from the M_w 8.2 event is observable above noise (Figure 4). Modulation, however, is less obvious. Lower amplitude of the body waves relative to the previous M_w 8.6 event may be responsible for the lack of clear modulation. Temporal evolution of state of stress surrounding the tremor source region may also play a significant role. We also find that there is a fairly impulsive start of the energy packet associated with *PKIKP* (i.e., high-frequency teleseismic compressional waves). We carefully inspected the high-frequency signal at stations with increasing distance from the modulated tremor source (Figure S2). It confirms two critical points: (1) Regardless of the distance from the tremor source, a high-frequency signal during *PKIKP* phases is recorded at all stations. This clearly suggests that the energy is teleseismic and therefore not tremor. (2) Tremor recorded during *S* wave phases shows up only at the stations close to the source locations and completely fades far away from the tremor source. This confirms the local origin of the signal radiating from tremor sources.

4. Discussion

It has been reported that tremor activity is extremely sensitive to small stresses imparted by earth tides and the passage of seismic waves from distant earthquakes. To understand the physics behind the dynamic modulating phenomenon, defining the critical modulating stress level is important. Reported critical stress perturbations are about 1–10 kPa for seismic waves [*Peng et al*., 2009; *Gomberg*, 2010] and about 9–35 kPa for tides [*Thomas et al*., 2009]. These values are close to the estimated stress drop of ETS events [*Miyazaki et al*., 2006]. The calculated dynamic stress transients on the Cascadia subduction thrust from the PGC data (σ_d = ~1.4 kPa for Love waves, ~4.2 kPa for Rayleigh waves, and ~0.7 kPa for SS body waves) for the M_w 8.6 earthquake are much higher than the reported critical stress perturbations, and hence, even the small stresses imparted by the body waves could modulate tremors in the central Vancouver region. Tremor is found to be modulated typically by surface waves. Triggering by body waves is less common. However, 0.8 kPa stress introduced by teleseismic *P* waves has triggered tremor at San Andreas Fault [*Ghosh et al*., 2009]. Hence, modulation of tremor by teleseismic *S* waves introducing ~0.7 kPa stress is clearly plausible and consistent with high stress sensitivity of tremor.

For the surface wave triggering, Love wave is characterized by higher triggering potential in this case. In the framework of Coulomb stress triggering and Mohr's circle, near-strike-parallel incidence wave, such as this case, along northern Cascadia has higher triggering potential [*Hill*, 2012]. Hence, it is not surprising to observe tremor modulation during Love waves. Modulation, however, continues well into the Rayleigh wave train, which has minimal triggering potential for the given geometry. Ongoing tremor swarm may help tremor modulation to continue even when the state of dynamic stress is not ideal.

Elevated tremor activity during the passage of teleseismic waves of the M_w 8.6 event does suggest that accelerated slip may have been triggered by the dynamic stresses. Even though stress magnitudes are toward the lower end of the spectrum, triggering in the present case may be easier because of the ongoing tremor swarm. Modulation of tremor in the form of tremor-beating observed over time scales of minutes is quite spectacular, indicating a fault's relatively quick response to transient stress pulses. Accelerated slip during the stress pulses can explain such tremor-beating. It is also possible that more tremor patches are brought to failure during each stress pulse. Interestingly, tremor-beating is not apparent during the passage

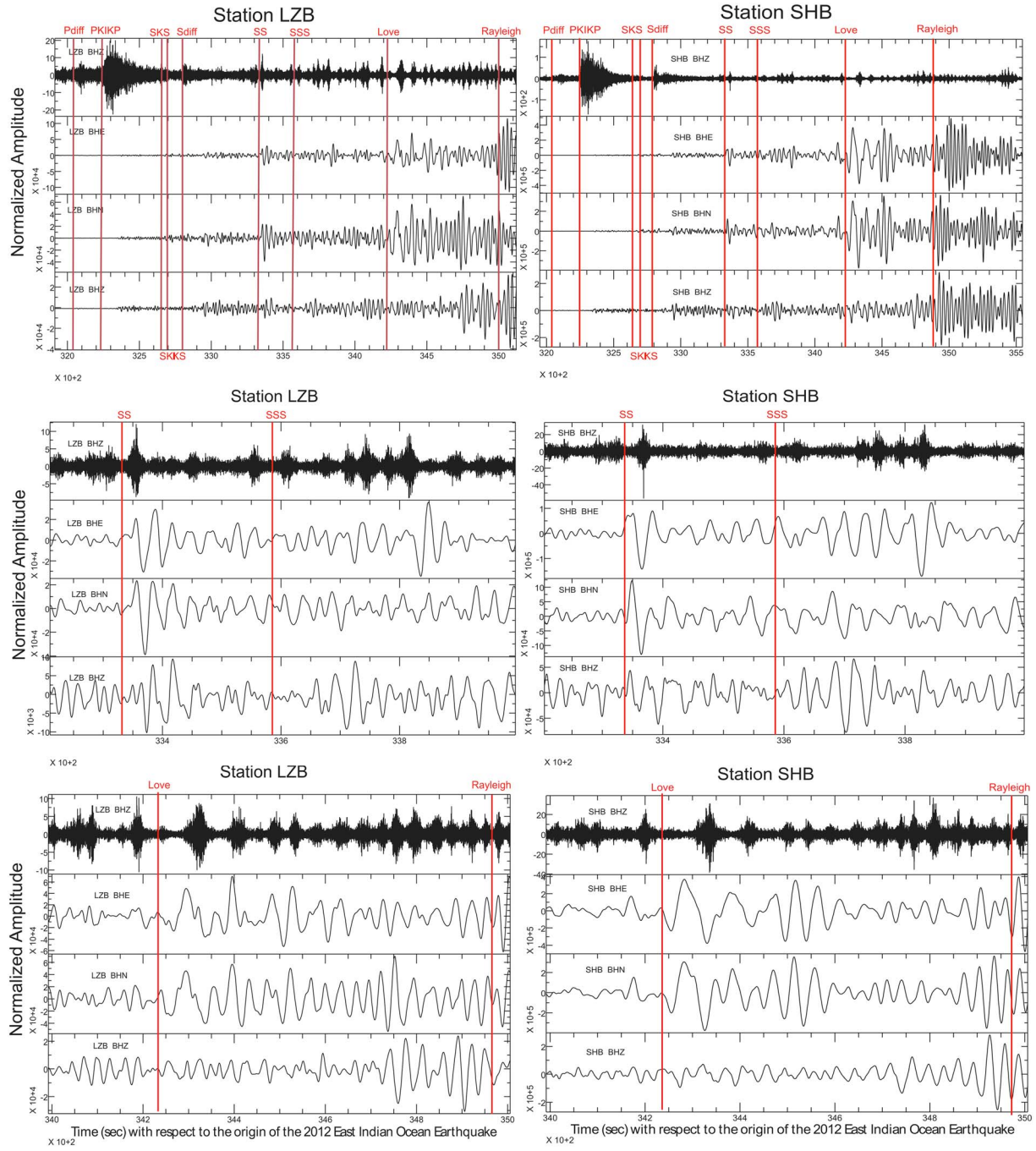

Figure 5. Seismograms for two best stations (LZB and SHB) to observe modulating tremor during arrival of *S* wave and surface waves. There are a total of six figures here, three for each station to showcase modulating tremor. Each figure has four row seismogram where the uppermost row is band passed at 2–4 Hz for the *Z* component, while the third rows below it are low passed at 0.1 Hz for all three components. Instrument response has not been removed so the amplitude is in counts. The seismograms are time-corrected based on the average tremor locations.

of teleseismic *P* waves but becomes clear after the arrival of shear waves. Relatively higher amplitude of shear waves suggests that *P* waves may have not introduced enough stress to influence the tremor sources.

5. Conclusions

So far in most cases, the surface waves are believed to be responsible for remote triggering and modulation of tremors [*Gomberg*, 2010; *Peng et al*., 2009; *Chao and Obara*, 2015]. Only a few cases have been reported of

triggering due to body waves [*Ghosh et al*., 2009; *Shelly et al*., 2011]. Here we report evidence for clear modulation of tectonic tremors in the Cascadia subduction zone near Vancouver Island by the teleseismic shear (body) wave phases, generated by the 11 April 2012, M_w 8.6 East Indian Ocean earthquake. The rate of tremor activity of an ongoing inter-ETS sequence increased by 1.5 times during the passage of seismic waves of the 11 April 2012, M_w 8.6, East Indian Ocean earthquake. The tremor modulation continued during the passage of the surface waves, and after that it was abruptly terminated and tremor activity returned to the background rate of the ongoing tremor episode. We estimate that ~0.7 kPa dynamic stress is introduced by the *S* body waves of the 11 April 2012, M_w 8.6, East Indian Ocean earthquake. This tiny stress is enough to significantly modulated tremor activity in the Vancouver Island region of northern Cascadia. Interestingly, modulated tremor shows slip-parallel streaking activity indicating interaction between accelerated slow slip front and fault plane structure. Similar modulation is observed during the passage of the waves from the M_w 8.2 event, which occurs 2 h later.

Acknowledgments

Borehole strainmeter and seismometer data used in this paper can be found at the Plate Boundary Observatory (PBO) archive hosted by UNAVCO, http://pbo.unavco.org/. Tremor catalog data used in this paper are archived by the Pacific Northwest Seismic Network (PNSN) and can be found at http://www.pnsn.org/tremor/. Broadband seismogram data used in this paper are archived by the Canadian National Seismograph Network and can be found at http://www.earthquakescanada.nrcan.gc.ca/stndon/CNSN-RNSC/index-eng.php. We thank Editor Jeroen Ritsema and two reviewers Kevin Chao and Chastity Aiken for constructive review and helpful discussion.

References

Aiken, C., Z. Peng, and K. Chao (2013), Tremors along the Queen Charlotte Margin triggered by large teleseismic earthquakes, *Geophys. Res. Lett.*, *40*, 829–834, doi:10.1002/grl.50220.

Bartlow, N. M., D. A. Lockner, and N. M. Beeler (2012), Laboratory triggering of stick-slip events by oscillatory loading in the presence of pore fluid with implications for physics of tectonic tremor, *J. Geophys. Res.*, *117*, B11411, doi:10.1029/2012JB009452.

Brudzinski, M. R., and R. M. Allen (2007), Segmentation in episodic tremor and slip all along Cascadia, *Geology*, *35*, 907–910, doi:10.1130/G23740A.1.

Chao, K., and K. Obara (2015), Triggered tectonic tremor in various types of fault systems of Japan following the 2012 Mw8.6 Sumatra earthquake, *J. Geophys. Res. Solid Earth*, *121*, 170–187, doi:10.1002/2015JB012566.

Chao, K., Z. Peng, H. Gonzalez-Huizar, C. Aiken, B. Enescu, H. Kao, A. A. Velasco, K. Obara, and T. Matsuzawa (2013), Global search of triggered tremor following the 2011Mw 9.0 Tohoku-Oki earthquake, in 2011 Tohoku earthquake and tsunami, *Bull. Seismol. Soc. Am.*, *103*, 1551–1571, doi:10.1785/0120120171.

Chlieh, M., et al. (2007), Coseismic slip and afterslip of the Great (Mw 9.15) Sumatra-Andaman earthquake of 2004, *Bull. Seismol. Soc. Am.*, *97*(1A), S152–S173.

Delahaye, E. J., J. Townend, M. E. Reyners, and G. Rogers (2009), Microseismicity but no tremor accompanying slow slip in the Hikurangi subduction zone, New Zealand, *Earth Planet. Sci. Lett.*, *227*, 21–28.

Delescluse, M. N., et al. (2012), April 2012 intra-oceanic seismicity off Sumatra boosted by the Banda-Aceh megathrust, *Nature*, *490*, 240–244, doi:10.1038/nature11520.

Delorey, A. A., K. Chao, K. Obara, and P. A. Johnson (2015), Cascading elastic perturbation in Japan due to the 2012 Mw8.6 Indian Ocean Earthquake, *Sci. Adv.*, *1*, e1500468.

Dragert, H., G. C. Rogers, J. Cassidy, H. H. Kao, and K. Wang (2004), Episodic tremor and slip in northern Cascadia, U.S. Geol. Surv. Prog. Rep. 04HQGR0047, pp. 1–6.

Ghosh, A., J. E. Vidale, Z. Peng, K. C. Craeger, and H. Houston (2009), Complex nonvolcanic tremor near Parkfield, California, triggered by the great 2004 Sumatra earthquake, *J. Geophys. Res.*, *114*, B00A15, doi:10.1029/2008JB006062.

Ghosh, A., J. E. Vidale, J. R. Sweet, K. C. Creager, A. G. Wech, H. Houston, and E. E. Brodsky (2010), Rapid, continuous streaking of tremor in Cascadia, *Geochem. Geophys. Geosyst.*, *11*, Q12010, doi:10.1029/2010GC003305.

Ghosh, A., J. E. Vidale, and K. C. Creager (2012), Tremor asperities in the transition zone control evolution of slow earthquakes, *J. Geophys. Res.*, *117*, B10301, doi:10.1029/2012JB009249.

Ghosh, A., E. Huesca-Pérez, E. E. Brodsky, and Y. Ito (2015), Very low frequency earthquakes in Cascadia migrate with tremor, *Geophys. Res. Lett.*, *42*, 3228–3232, doi:10.1002/2015GL063286.

Gomberg, J. (2010), Lessons from (triggered) tremor, *J. Geophys. Res.*, *115*, B10302, doi:10.1029/2009JB00711.

Graindorge, D., et al. (2008), Impact of lower plate structure on upper plate deformation at the NW Sumatran convergent margin from seafloor morphology, *Earth Planet. Sci. Lett.*, *275*, 201–210.

Hawthorne, J. C., and A. M. Rubin (2010), Tidal modulation of slow slip in Cascadia, *J. Geophys. Res.*, *115*, B09406, doi:10.1029/2010JB007502.

Hill, D. P. (2012), Surface-wave potential for triggering tectonic (nonvolcanic) tremor Corrected, *Bull. Seismol. Soc. Am.*, *102*(6), 2313–2336, doi:10.1785/0120120085.

Houston, H., B. G. Delbridge, A. G. Wech, and K. C. Creager (2011), Rapid tremor reversals in Cascadia generated by weakened plate interface, *Nat. Geosci.*, *4*(6), 404–409, doi:10.1038/Ngeo1157.

Ide, S., D. R. Shelly, and G. C. Beroza (2007), The mechanism of deep low frequency earthquakes: Further evidence that deep non-volcanic tremor is generated by shear slip on the plate interface, *Geophys. Res. Lett.*, *34*, L03308, doi:10.1029/2006GL028890.

Ishii, M., E. Kiser, and E. L. Geist (2013), Mw 8.6 Sumatran earthquake of 11 April 2012: Rare seaward expression of oblique subduction, *Geology*, *41*, 319–322.

Johnson, C. W., and R. Bürgmann (2015), Delayed dynamic triggering: Local seismicity leading up to three remote M ≥ 6 aftershocks of the 11 April 2012 M8.6 Indian Ocean earthquake, *J. Geophys. Res. Solid Earth*, *120*, 134–151, doi:10.1002/2015JB012243.

Kiser, E. (2012), Preliminary rupture modelling of the April 11, 2012 Sumatran earthquakes. [Available at http://www.seismology.harvard.edu/research_sumatra2012.html.]

Mazzotti, S., and J. Adams (2004), Variability of near-term probability for the next great earthquake on the Cascadia subduction zone, *Seismol. Soc. Am. Bull.*, *94*, 1954–1959, doi:10.1785/012004032.

McGuire, J., and G. Beroza (2012), A rogue earthquake off Sumatra, *Science*, *336*, 1118–1119.

Meng, L., J.-P. Ampuero, Z. Duputel, Y. Luo, and V. C. Tsai (2012), Earthquake in a maze: Compressional rupture branching during the 2012 Mw 8.6 Sumatra earthquake, *Science*, *337*, 724–726.

Miyazaki, S., P. Segall, J. J. McGuire, T. Kato, and Y. Hatanaka (2006), Spatial and temporal evolution of stress and slip rate during the 2000 Tokai slow earthquake, *J. Geophys. Res.*, *111*, B03409, doi:10.1029/2004JB003426.

Miyazawa, M. (2012), Detection of seismic events triggered by P-waves from the 2011 Tohoku-Oki earthquake, *Earth Planets Space*, *64*(12), 1223–1229, doi:10.5047/eps.2012.07.003.

Obara, K. (2002), Nonvolcanic deep tremor associated with subduction in southwest Japan, *Science*, *296*, 1679–1681.

Obara, K., H. Hirose, F. Yamamizu, and K. Kasahara (2004), Episodic slow slip events accompanied by non-volcanic tremors in southwest Japan subduction zone, *Geophys. Res. Lett.*, *31*, L23602, doi:10.1029/2004GL020848.

Peng, Z., and J. Gomberg (2010), An integrated perspective of the continuum between earthquakes and slow slip phenomena, *Nat. Geosci.*, *3*, 399–607, doi:10.1038/ngeo940.

Peng, Z., J. E. Vidale, A. G. Wech, R. M. Nadeau, and K. C. Creager (2009), Remote triggering of tremor along the San Andreas Fault in central California, *J. Geophys. Res.*, *114*, B00A06, doi:10.1029/2008lB006049.

Pollitz, F., R. S. Stein, V. Sevilgen, and R. Burgmann (2012), The 11 April 2012 east Indian Ocean earthquake triggered large aftershocks worldwide, *Nature*, *490*, 250–253, doi:10.1038/nature11504.

Rubinstein, J. L., J. E. Vidale, J. Gomberg, P. Bodin, K. C. Creager, and S. D. Malone (2007), Non-volcanic tremor driven by large transient shear stresses, *Nature*, *448*, 579–582.

Rubinstein, J. L., J. Gomberg, J. E. Vidale, A. G. Wech, H. Kao, K. C. Creager, and G. Rogers (2009), Seismic wave triggering of nonvolcanic tremor, episodic tremor and slip, and earthquakes on Vancouver Island, *J. Geophys. Res.*, *114*, B00A01, doi:10.1029/2008JB005875.

Shelly, D. R., G. C. Beroza, and S. Ide (2007), Non-volcanic tremor and low-frequency earthquake swarms, *Nature*, *446*, 305–307.

Shelly, D. R., Z. Peng, D. R. Hill, and C. Aiken (2011), Triggered creep as a possible mechanism for dynamic triggering of tremor and earthquakes, *Nat. Geosci.*, *4*, 384–388.

Thomas, A. M., R. M. Nadeau, and R. Burgmann (2009), Tremor-tide correlations and near-lithostatic pore pressure on the deep San Andreas fault, *Nature*, *462*, 1048–1051, doi:10.1038/nature08654.

Thomas, T. W., J. E. Vidale, H. Houston, K. C. Creager, J. R. Sweet, and A. Ghosh (2013), Evidence for tidal triggering of high-amplitude rapid tremor reversals and tremor streaks in northern Cascadia, *Geophys. Res. Lett.*, *40*, 4254–4259, doi:10.1002/grl.50832.

Vidale, J. E., A. J. Hotovec, A. Ghosh, K. C. Creager, and J. Gomberg (2011), Tiny intraplate earthquakes triggered by nearby episodic tremor and slip in Cascadia, *Geochem. Geophys. Geosyst.*, *12*, Q06005, doi:10.1029/2011GC003559.

Wang, D., J. Mori, and S. Ohmi (2012), Rupture process of the April 11, 2012 Sumatra (Mw 8.6) earthquake imaged with back-projection of Hi-net data. [Available at http://www.eqh.dpri.kyoto-u.ac.jp/src/etc/sumatra.htm.]

Wech, A. G., and K. C. Creager (2011), A continuum of stress, strength and slip in the Cascadia subduction zone, *Nat. Geosci.*, *4*, 624–628, doi:10.1038/ngeo1215.

Wiseman, K., and R. Bürgmann (2012), Stress triggering of the great Indian Ocean strike-slip earthquakes in a diffuse plate boundary zone, *Geophys. Res. Lett.*, *39*, L22304, doi:10.1029/2012GL053954.

Yadav, R. K., B. Kundu, K. Gahalaut, J. Catherine, V. K. Gahalaut, A. Ambikapthy, and M. S. Naidu (2013), Coseismic offsets due to the April 11, 2012 Indian Ocean earthquakes (Mw 8.6 and 8.2) derived from GPS measurements, *Geophys. Res. Lett.*, *40*, 3389–3393, doi:10.1002/grl.50601.

Yue, H., T. Lay, and K. D. Koper (2012), En-echelon and orthogonal fault ruptures of the 11 April 2012 great interplate earthquake, *Nature*, *490*, 245–249, doi:10.1038/nature11492.